
Deep Convolutional Inverse Graphics Network

Tejas D. Kulkarni^{*1}, Will Whitney^{*2}, Pushmeet Kohli³, Joshua B. Tenenbaum⁴

^{1,2,4}Computer Science and Artificial Intelligence Laboratory, MIT

^{1,4}Brain and Cognitive Sciences, MIT

³Microsoft Research Cambridge, UK

¹tejask@mit.edu ²wwhitney@mit.edu ³pkohli@microsoft.com ⁴jbt@mit.edu

** First two authors contributed equally to this work.*

Abstract

This paper presents the Deep Convolution Inverse Graphics Network (DC-IGN) that aims to learn an interpretable representation of images that is disentangled with respect to various transformations such as object out-of-plane rotations, lighting variations, and texture. The DC-IGN model is composed of multiple layers of convolution and de-convolution operators and is trained using the Stochastic Gradient Variational Bayes (SGVB) algorithm [12]. We propose training procedures to encourage neurons in the *graphics code* layer to have semantic meaning and force each group to distinctly represent a specific transformation (pose, light, texture, shape etc.). Given a static face image, our model can re-generate the input image with different pose, lighting or even texture and shape variations from the base face. We present qualitative and quantitative results of the model's efficacy to learn a 3D rendering engine. Moreover, we also utilize the learnt representation for two important visual recognition tasks: (1) an invariant face recognition task and (2) using the representation as a summary statistic for generative modeling.

1 Introduction

Deep learning has led to remarkable breakthroughs in automatically learning hierarchical representations from images. Models such as Convolutional Neural Networks (CNNs) [16, 13], Restricted Boltzmann Machines (RBM) based generative models [9, 24, 17], and Auto-encoders [1, 28, 20] have been successfully applied to produce multiple layers of increasingly abstract visual representations. However, there is relatively little work on characterizing what is the optimal representation of the data. While researchers such as Cohen *et al.* [6] have considered this problem by proposing a theoretical framework to learn irre-

ducible representations having both invariances and equivariances, coming up with the best representation for any given task is an open question.

The Vision as inverse graphics approach offers an interesting perspective to various desiderata for a good representation [2, 6, 8]: invariance, meaningfulness of representations, abstractions and disentanglement. Computer graphics is a function to go from compact description of scenes (*graphics code*) to images. This *graphics code* based representation is often disentangled to allow rendering scenes with fine-grained control over transformations such as object location, pose, lighting, texture and shape. Therefore, it naturally produces representations satisfying the above-mentioned properties.

Recent work in inverse graphics [11, 19, 18, 14] follows a general strategy of first defining a probabilistic or non-probabilistic model with latent parameters, followed by an inference or optimization algorithms to find the most appropriate set of latent parameters given observations. Recently, Tieleman *et al.* [26] moved beyond this two stage pipeline by using a generic encoder network with a domain-specific decoder network to approximate a 2D rendering function. However, none of these approaches have been demonstrated to automatically produce a semantically interpretable *graphics code* and to learn an approximate 3D rendering engine to re-produce images.

In this paper, we present an approach for learning interpretable *graphics codes*. Given a set of images, we use a hybrid encoder-decoder model (trained using unsupervised and/or semi-supervised learning) to learn a representation that is disentangled with respect to various transformations such as object out-of-plane rotations, lighting variations, texture and subtle changes in 3D geometry. To achieve this, we employ a deep directed graphical model with many layers of convolution and de-convolution operators that is trained using the Stochastic Gradient Variational Bayes (SGVB) algorithm [12]. Without the loss of generality, we present 3D face analysis as a working example throughout this paper. We choose faces due to their rich intrinsic shape and appearance variability. Moreover, ac-

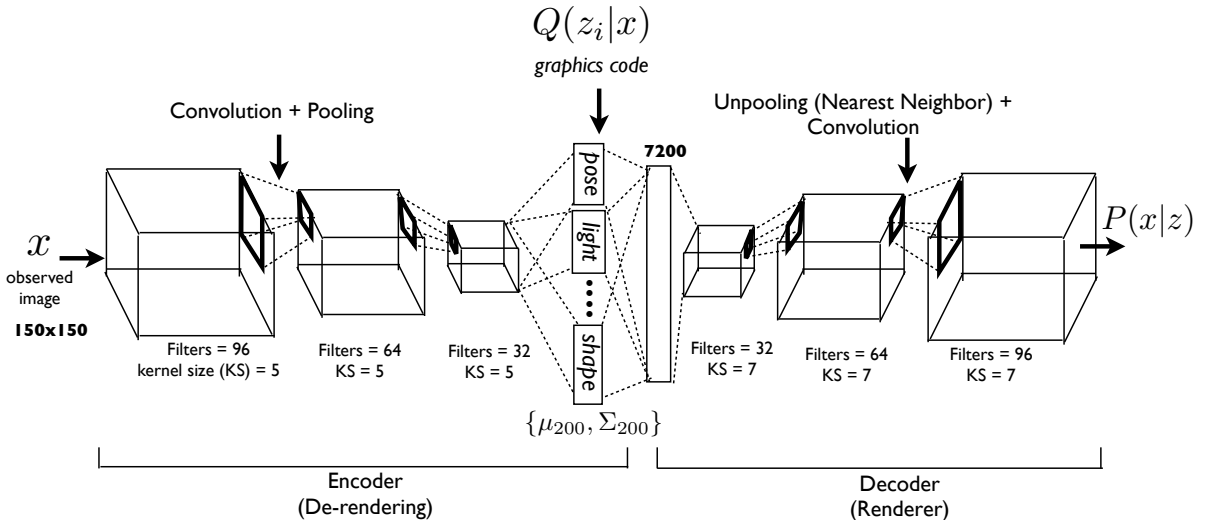


Figure 1: **Model Architecture:** Deep Convolutional Inverse Graphics Network (DC-IGN) has an encoder and a decoder. We follow the variational autoencoder[12] architecture with several variations. The encoder consists of several layers of convolutions followed by max-pooling and the decoder has several layers of unpooling (upsampling using nearest neighbors) followed by convolution. (a) During training, data x is passed through the encoder to produce the posterior approximation $Q(z_i|x)$, where z_i consists of scene latent variables such as pose, light, texture or shape. In order to learn parameters in DC-IGN, gradients are backpropagated using stochastic gradient descent using the following variational object function: $-\log(P(x|z_i)) + KL(Q(z_i|x)||P(z_i))$ for every z_i . We can force DC-IGN to learn a disentangled representation by showing mini-batches with a set of inactive and active transformations (eg face rotating, light sweeping in some direction etc). (b) During test, data x can be passed through the encoder to get latents z_i . Images can be re-rendered to different viewpoints, lighting conditions, shape variations etc by just manipulating the appropriate graphics code group (z_i), which is how one would manipulate an off the shelf 3D graphics engine.

cess to large number of training data allows us to carefully tease apart the effects of training size, learning algorithm and modeling biases.

We propose various training procedures to encourage neurons in the *graphics code* layer to have semantic meaning and forces each group to distinctly represent a specific transformation (pose,light,texture,shape etc.). To learn a disentangled representation, we train with random variations on different transformations in each mini-batch of data. Another approach we adopt is to train using data where each mini-batch has a set of active and inactive transformations (but we do not provide target values as in supervised learning). For example, a nodding face would have the 3D elevation transformation active but its shape, texture and other affine transformations would be inactive. We exploit this type of a learning procedure to force chosen neurons in the *graphics code* layer to specifically represent active transformations, thereby automatically creating a disentangled representation. Given a static face image, our model can re-generate the input image with different pose, lighting or even texture and shape variations from the base face. We present qualitative and quantitative results of the model’s efficacy to learn a 3D rendering engine. Moreover, we also utilize the learnt representation for two important visual recognition tasks: (1) an invariant face recognition task and (2) using the representation as a summary statistic

for generative modeling.

2 Related Work

As mentioned before, a number of generative models have been proposed in the literature to obtain abstract visual representations. Unlike most RBM based models[9, 24, 17], our approach is trained using back-propagation from the data reconstruction term and the variational bound.

Relatively recently, Kingma *et al.* [12] proposed the SGVB algorithm to learn generative models with continuous latent variables. In this work, a feed-forward neural network (encoder) is used to approximate the posterior distribution and a decoder network serves to enable stochastic reconstruction of observations. In order to handle fine-grained geometry of faces, we work with relatively large scale images (150x150). Therefore, our approach extends and applies the SGVB algorithm to jointly train and utilize many layers of convolution and de-convolution operators for the encoder and decoder network respectively. The decoder network is a function that transform a compact *graphics code* (200 dimensions) to a 150x150 image. We propose using unpooling (nearest neighbor sampling) followed by convolution to handle the massive increase in dimensionality while keeping the number of parameters be bounded. Generative stochastic networks [3] which learn the transi-

tion operator of a Markov chain whose stationary distribution samples from the data distribution are also relevant to our work. Recently, [7] proposed using CNNs to generate images given object-specific parameters in a supervised setting. As their approach requires ground-truth labels for the *graphics code* layer, it cannot be directly applied to image interpretation tasks. Our work is also similar in spirit to [25], but in comparison our model does not assume a lambertian reflectance model and implicitly constructs the 3D representations. Another piece of related work is the deconvolution network by Zeiler *et al.* [31] which is used to produce image representations using convolutional decomposition of images under a sparsity constraint.

In comparison to existing approaches, it is important to note that our encoder network produces interpretable and disentangled representations, which is necessary to learn a meaningful 3D graphics engine. A number of inverse graphics inspired methods have recently been proposed in the literature [11, 19, 18]. However, most such methods rely on hand-crafted rendering engines. The exception to this is work by Hinton *et al.* [10] (*transforming autoencoders*) and Tieleman [26] which uses a domain specific decoder to reconstruct input images. Our work is similar in spirit to these works but has some key differences: (a) It uses a very generic convolutional architecture in the encoder and decoder networks to enable efficient learning on large datasets and image sizes, (b) it can handle single static frames as opposed to pair of images required in [10], and (c) it is generative.

3 Model

As shown in figure 1, the basic structure of the Deep Convolutional Inverse Graphics Network (DC-IGN) consists of: the encoder network that captures distribution over *graphics codes* Z given data x and a decoder network which learns the conditional distribution to produce \hat{x} given Z . Z can be a disentangled representation containing several factored set of latent variables $z_i \in Z$ such as pose, light and shape. This is important to learn a meaningful approximation of a 3D graphics engine and helps tease apart the generalization capability of the model with respect to different types of transformations on static images.

Let us denote the encoder output of DC-IGN to be $y_e = \text{encoder}(x)$. The encoder output is used to parametrize the variational approximation $Q(z_i|y_e)$, where Q is chosen to be a multivariate normal distribution. There are two reasons for using this parametrization: (1) Gradients of samples with respect to parameters θ of Q can be easily obtained using the reparametrization trick proposed in [12], and (2) Various statistical shape models trained on 3D scanner data such as faces have the same multivariate normal latent distribution (see section 4.1). Given that model parameters W_e connect y_e and z_i , the distribution parameters

$$z = \begin{array}{|c|c|c|c|} \hline z_1 & z_2 & z_3 & z_{[4,n]} \\ \hline \end{array}$$

corresponds to $\phi \quad \alpha \quad \phi_L$ intrinsic properties (shape, texture, etc)

Figure 3: **Structure of the representation vector.** ϕ is the azimuth of the face, α is the elevation of the face with respect to the camera, and ϕ_L is the azimuth of the light source.

$\theta = (\mu_{z_i}, \Sigma_{z_i})$ and latents Z can then be expressed as:

$$\mu_{z_i} = W_e * y_e \tag{1}$$

$$\Sigma_{z_i} = \text{diag}(\exp(W_e * y_e)) \tag{2}$$

$$\forall i, z_i \sim \mathcal{N}(\mu_{z_i}, \Sigma_{z_i}) \tag{3}$$

We present several training procedures for DC-IGN to learn representations with different characteristics:

3.1 Random Transformations

For our simplest training procedure, we construct minibatches of randomly selected training samples and train the DC-IGN network in figure 1 according to the SGVB procedure. This training leads to networks with extremely strong reconstruction performance. We explore several uses of the representations generated by these networks in section 4.

3.2 Specific Transformations

One of the main goals of this work is for the DC-IGNs to learn a representation of the data which consists of disentangled and semantically interpretable latent variables. Following Bengio *et al.*[2] we would like only a small subset of the latent variables to change for sequences of inputs corresponding to real-world events.

One natural choice of target representation for information about scenes is that already designed for use in graphics engines. If we can deconstruct a face image by splitting it into variables for pose, light, and shape, we can trivially represent the same kinds of transformations that these variables are used for in graphics applications. Figure 3 depicts the representation which we will attempt to learn.

To achieve this goal, we perform a training procedure which directly targets this definition of disentanglement. We organize our data into minibatches corresponding to changes in only a single scene variable (azimuth angle, elevation angle, and azimuth angle of the light source); these are transformations which might occur in the real world. We will term these the extrinsic variables. To train this representation, we adopt a procedure that is similar to SGVB, with the key differences being:

1. Select at random a latent variable z_{train} which we

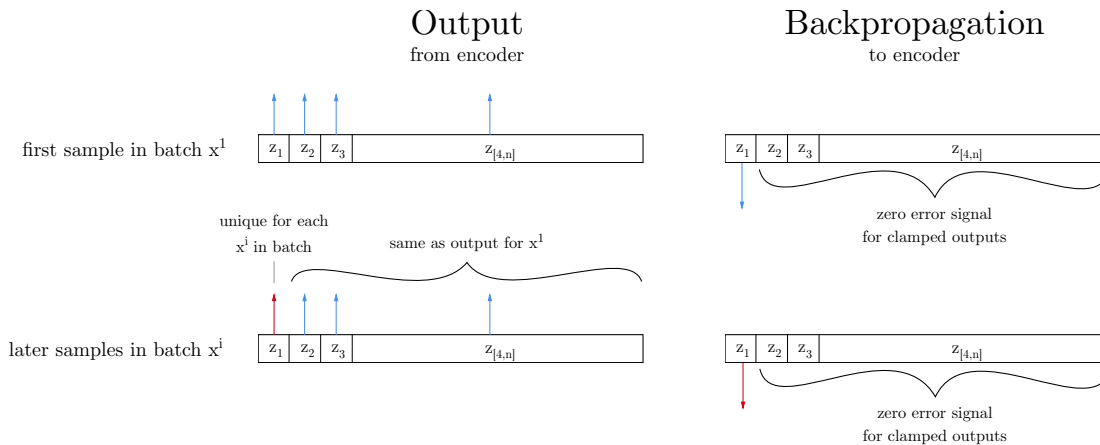


Figure 2: **Training on a minibatch in which only ϕ , the azimuth angle of the face, changes.** During the forward step, the output from each component $z_k \neq z_1$ of the encoder is forced to be the same for each sample in the batch. This reflects the fact that the generating variables of the image which correspond to the desired values of these latents are unchanged throughout the batch. By holding these outputs constant throughout the batch, z_1 is forced to explain all the variance within the batch, i.e. the full range of changes to the image caused by changing ϕ . During the backward step, backpropagation of gradients happens only through the latent z_1 , with gradients for $z_k \neq z_1$ set to zero. This corresponds with the clamped output from those latents throughout the batch.

wish to correspond to one of {azimuth angle, elevation angle, azimuth of light source}

2. Select at random a minibatch in which that extrinsic scene variable changes
3. Show the network the first example in the minibatch and capture its latent representation z^1
4. For all subsequent examples in the minibatch, hold all $z_i \neq z_{train}$ constant and equal to z_i^1 (these latents are "clamped")
5. Backpropagate error as usual in the decoder, but pass zero gradients for all $z_i \neq z_{train}$. The gradient at z_i should be passed through unchanged.
6. Continue backpropagation through the encoder using the modified gradient.

Along with these we generate minibatches in which the three extrinsic scene variables are held fixed but all other properties of the image (variables controlling the identity and appearance of the face) change randomly. These intrinsic properties of the model are represented by the remainder of the latent variables. Training of these remaining latent variables is similar to the procedure above, but instead of a single element being trained, $z_{train} = z_{[4,n]}$. That is, we clamp the latent variables corresponding to the extrinsic properties of pose and lighting and only allow the intrinsic latents $z_{[4,n]}$ to change within a batch; they are similarly the only latents given nonzero gradients. These minibatches varying intrinsic properties are interspersed stochastically with those varying the extrinsic properties. The probability

of selecting an intrinsic batch is proportional to a hyperparameter we term the "shape bias", for it represents a "bias" in the training set towards examples which vary the underlying shape of the face.

This training method leads to networks whose latent variables have a strong *equivariance* with the generating parameters, as shown in figure 9. This allows the value of the true generating parameter to be trivially extracted from the latent representation. However, this training method does not directly enforce the *invariance* of the clamped latents to transformations to which one might like them to be insensitive. Instead, it gets its invariances from the tendency of neural networks' representations to approach locally optimal compression. Since information about, for example, the elevation of the face is explicitly required to be stored in z_2 , any information about the elevation stored in any other z_i would be redundant and wasteful of that z_i 's information-carrying capacity.

3.2.1 Invariance targeting

In order to further improve the invariance of the procedure defined in section 3.2, we propose a procedure for explicitly training invariance of the latent variables to orthogonal transformations. As depicted in figure 4, we replace the zero gradients of the $z_i \neq z_{train}$ from section 3.2 with an error gradient pointing in the direction of greatest difference from the mean of the latent variables we desire to be invariant in this minibatch. During training, this pushes the values which we desire to be constant throughout the batch towards one another, decreasing the variation that these latents experience due to orthogonal variables. This regularizing force needs to be scaled to be much smaller than the

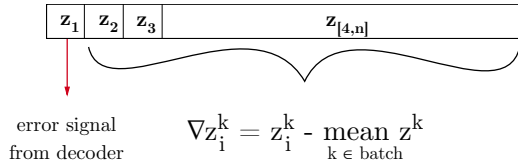


Figure 4: **Backpropagation with invariance targeting.** In order to directly enforce invariance of the latents corresponding to properties of the image which do not change within a given batch, we calculate gradients for each z^k predicted latent in the batch which moves it towards the mean of each invariant latent over the batch. This is equivalent to regularizing the latents $z_{[2,n]}$ by the L2 norm of $z^k - \text{mean}_{k \in \text{batch}} z^k$.

true training signal; empirically, a factor of 1/100 works well.

4 Experiments

We experimented with two common visual perception tasks: (1) invariant recognition task to predict whether two faces are same or equal, and (2) using the learnt DC-IGN representation as a distance metric in likelihood-free bayesian inference. These tasks stress the importance of a disentangled representation – given a factored set of z_i 's, invariance follows automatically by ignoring subsets of z_i 's. For face recognition, if we denote $z_{identity} \in \{z_{shape}, z_{texture}\}$ to be latents corresponding to facial identity and $\{z_{pose}, z_{light}\}$ to be rest of the variables, then we can extract an invariant represent of any given face by using $z_{identity}$ and ignoring all other z_i 's. Similarly, for using Z as a distance metric, we may wish to preserve all transformations to be equivariant by keeping all Z 's around.

Vetter et al.[5] first proposed using 3D laser scanned face data to learn a deformable 3D face model (3DMM). During training of 3DMM model, 3D faces are manually aligned to be in a canonical pose and a statistical shape based model is obtained with tunable vector based representation. In all our experiments, we train using the synthetic data obtained from the 3DMM model and test it out on real face data with ground truth 3D annotations (geometry and texture) obtained from [23]. This model allows us to generate synthetic images of faces by systematically varying pose, light, shape and texture. Moreover, 3DMM also gives us a good ground truth metric to test the generalization capabilities of our learnt 3D rendering function. We trained our model on about 10000 batches of faces, where each batch consists of about 30 faces on average with random variations on face identity variables (shape/texture), pose and lighting. We used *rmsprop*[26] learning algorithm during training and

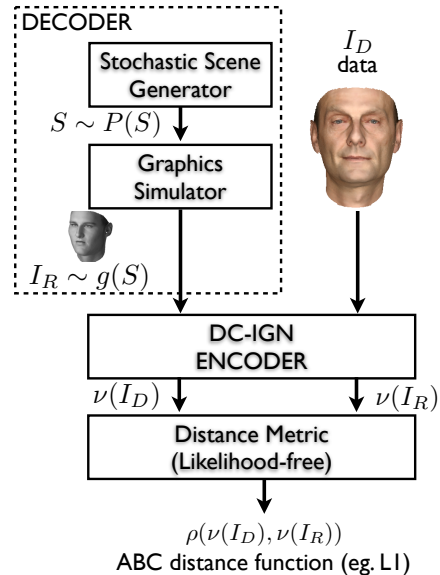


Figure 5: **Deep DC-IGN encoder with a domain-specific decoder:** In order to test the equivariance of DC-IGNs learnt representation, we can use DC-IGN encoder output as summary statistic for likelihood-free bayesian inference. We use the 3DMM Basel face model as prior on 3D faces. The prior $P(S)$ is a multivariate gaussian distribution which generates a set of latent variables S_i denoting pose, lighting, shape and texture. The scene S can be passed to a graphics simulator which produces the hypothesis image I_R . Given I_R and observation image I_D , the task is to infer $P(S|I_D)$. Since the likelihood function is not available in closed-form, we can simply resort to approximate Bayesian computation (ABC) based MCMC[29]. The DC-IGN encoder produces summary statistics for both the observation $\nu(I_D)$ and current hypothesis $\nu(I_R)$, where the current hypothesis is accepted or rejected.

set the meta learning rate to be equal to 0.0005, the momentum decay to be 0.1 and weight decay to be 0.01.

4.1 3D Statistical Shape Modeling

In order to test the equivariance power of DC-IGN's learnt representation, we use Z as a summary statistic in a generative model based on the 3DMM face model. Given a pre-trained DC-IGN, we are interested in the following question – how well can we recover latents of a compositional 3D shape model by using latent representations Z ? After convergence, this inference procedure produces 3D vertices and reflectance values for each vertex given a single static image. Intuitively, we are essentially using DC-IGN representations along with a rich domain-specific face decoder model for coarse-to-fine inference. Alternatively, we can also use the learnt representations from our model to learn data-driven proposals similar to [11].

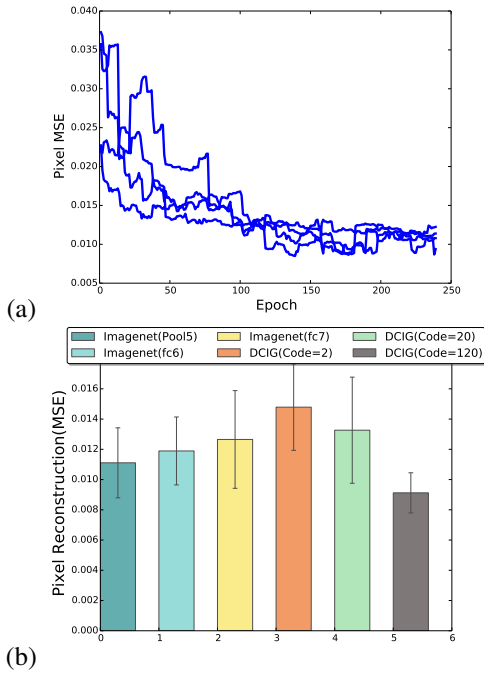


Figure 6: **3D Face generative model results:** (a) As inference for scheme highlighted in figure 5 proceeds, the pixel reconstruction error (MSE) between the observed image and the hypothesis I_R decreases. We show multiple independent chains to illustrate typical inference trajectories during inference. Note how the pixel error increases considerably during some of the intermediate runs but then converges to a lower value with more iterations, suggesting that it escapes some of the local minimas as it is following a smoother manifold in the DC-IGN’s representation space. (b) We quantitatively compared the test pixel reconstruction error for various baseline models – pre-trained Imagenet with different layers as the chosen summary statistic and DC-IGN with varying number of neurons in the *graphics code* layer.

Bayesian inference in our setting is difficult as the likelihood is unavailable in closed form due to the presence of the rendering pipeline and subsequent DC-IGN computations. However, there has been considerable progress in the statistics community to perform likelihood free Bayesian inference, which is often termed as Approximate Bayesian Computation (ABC). Therefore, ABC provides a natural formulation to describe inverse graphics in likelihood-free settings. We define a simple distance function on the summary statistics obtained from the DC-IGN-encoder networks and apply a variant of the probabilistic approximate MCMC algorithm [29] to do inference.

We used a pre-trained DC-IGN encoder-decoder network (from any one of the training procedures) on the synthetic face dataset, followed by stripping the decoder part of the network. The DC-IGN encoder can now be used as a sum-

mary statistic function $\nu : x \rightarrow Z$, which calculates the latent representation Z for any given image x . We replace the DC-IGN decoder network by a richer generative model based on the 3DMM face model. This is similar in spirit to Nair et al.[22], where a domain-specific decoder is used along with a generic encoder to do analysis-by-synthesis based generative modeling.

The 3DMM face model consists of a set of two face related latent variables ($S_{shape}, S_{texture}$), each with 200 dimensions and sampled from $\{\mathcal{N}(0, 1)\}_{i=1}^{200}$. Additionally, there are scene variables including: ($S_{light}, S_{elevation}$) $\sim Uniform(-90, 90)$ and $\{S_{camera}^j\}_{j \in \{x, y, z\}} \sim Uniform(0, 1)$. Let us denote $\mathbb{I}_B(\cdot)$ as the indicator function of the set B and $A_{\epsilon, I_D} = \{I_R | \rho(\nu(I_D), \nu(I_R)) \leq \epsilon\}$, where ρ can be a suitable distance metric such as L1. As shown in figure 5, $g(S)$ denotes the graphics simulator which generates rendering primitives (images, mesh, etc.) given a scene S . We can now formulate the image interpretation task as approximately sampling the posterior distribution of scene S given observations (I_D):

$$\pi(S|I_D) \approx \pi_{\epsilon}(S|I_D), \quad (4)$$

$$\text{where } \pi_{\epsilon}(S|I_D) \quad (5)$$

$$= \int \pi_{\epsilon}(S, I_R|I_D) dI_R \quad (6)$$

$$\propto \frac{\pi(S) \delta_g(S)(I_R) \mathbb{I}_{A_{\epsilon, I_D}}(I_R)}{\int_{A_{\epsilon, I_D} \times S} \pi(S) \delta_g(S)(I_R) dS} \quad (7)$$

During inference, we make use of elliptical proposals on large set of coupled continuous random variables S . Neal [4] and Murray et al. [21] studied generative models with Gaussian priors having zero mean and arbitrary covariance structure. Let us assume that $X \sim \mathcal{N}(0, \Sigma)$. Given a state S of the scene, a new state S' can be efficiently proposed as follows: $S' = \sqrt{1 - \alpha^2} S + \alpha \theta$, where $\theta \sim \mathcal{N}(0, \Sigma)$ and $\alpha \sim Uniform(-1, 1)$.

Based on figure 6(a), as inference proceeds the pixel difference between the current hypothesis of the model and observation decreases. We also quantitatively compare DC-IGN’s latent representation with a pre-trained deep convolutional network (trained on Imagenet [27] version: *imagenet-caffe-ref*). We used several intermediate layers of the pre-trained network as the summary statistics and show quantitative performance on test data in comparison to various DC-IGN models. The DC-IGN models were trained with different number of dimensions for Z . From figure 6(b), it is clear that DC-IGN code with a relatively larger dimensions is necessary to capture the rich set of transformations on real faces. This emphasizes the fact that to obtain a disentangled representation, data reconstruction through a small bottleneck *graphics code* layer might be more beneficial than just tuning for recognition as is the case with supervised CNNs.

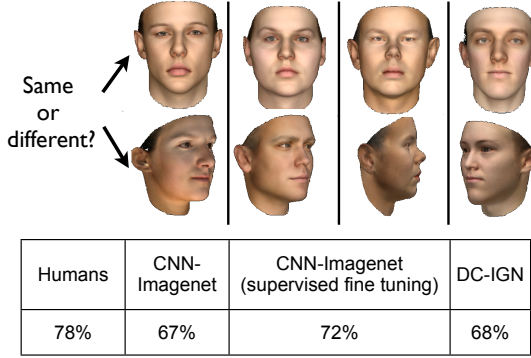


Figure 7: **Invariance Tests:** In order to test the invariance of Z , we tested the network on predicting whether a given pair of images has the same or different face. Due to pose-light variability, this task is hard even for human subjects (limited viewing time of about 200ms). We quantitatively compared the prediction task with a pre-trained Imagenet CNN and also a fine-tuned version of the same CNN with the face dataset (see section 4.2 for details). Both of these baselines were trained or fine-tuned with supervised learning. On the other hand, DC-IGN achieves comparable accuracy with just unsupervised learning.

4.2 Recognition

In order to test the invariance properties of DC-IGN, we performed a task to predict whether two given faces are same or different. This experiment was first proposed by Yildirim et al[30] and we closely follow this procedure for all neural network baselines.

The test dataset from Yildirim et al. consists of 96 pairs of faces with varying degree of pose, lighting, shape and texture. In order to ensure that the task is interesting and hard, they also obtained accuracy of the prediction from human subjects using Amazon Turk. Obtaining an invariant representation is hard as the two faces can have drastically different transformations. We also obtained a fine-tuned CNN on the SURF-W dataset from Yildirim et al., which was fine-tuned with 400 famous people under different light-pose conditions. As shown in figure 7, humans perform at 78 percent which is higher than all deep learning based system. It is perhaps surprising that DC-IGN performs competitively with other baseline models even when trained completely unsupervised using the *random transform* training procedure in section 3.1.

In order to calculate test accuracy of the *same vs different* task for all baseline models, we follow the same-vs-different test procedure first proposed in [30]. We first scaled each test image representation independently to be centered at 0 and to have a standard deviation of 1. Then, for each pair of images, we calculated the Pearson correlation coefficient between the two network representations. We searched for a threshold correlation $\in [1, 1]$ such that

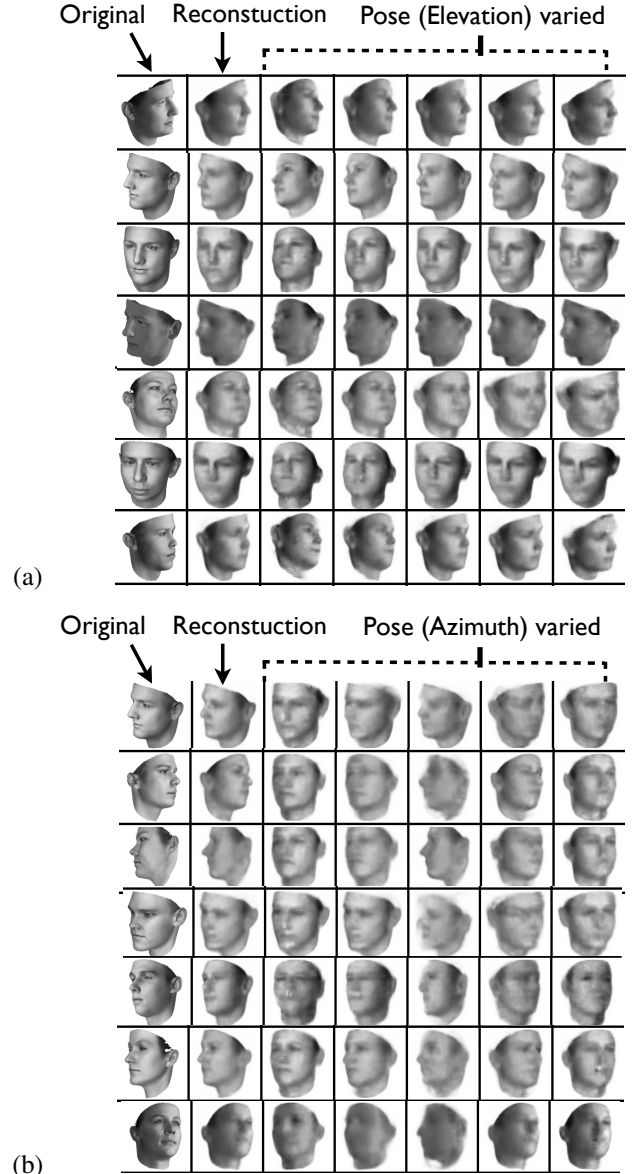


Figure 8: **Manipulating pose variables:** Qualitative results showing the generalization capability of the learnt DC-IGN decoder to render original static image with different pose directions.(a) The latent neuron $z_{elevation}$ is changed to random values but all other latents are clamped. (b) The latent neuron $z_{azimuth}$ is changed to random values but all other latents are clamped.

the any given model’s performance will be highest with respect to ground truth. The search was such that the pairs of correlation values lower than the threshold were assigned *different*, and the pairs of equal or higher correlation values than the threshold were assigned *same* by the model. We report results based upon the threshold that gives the highest performance for each baseline model separately.

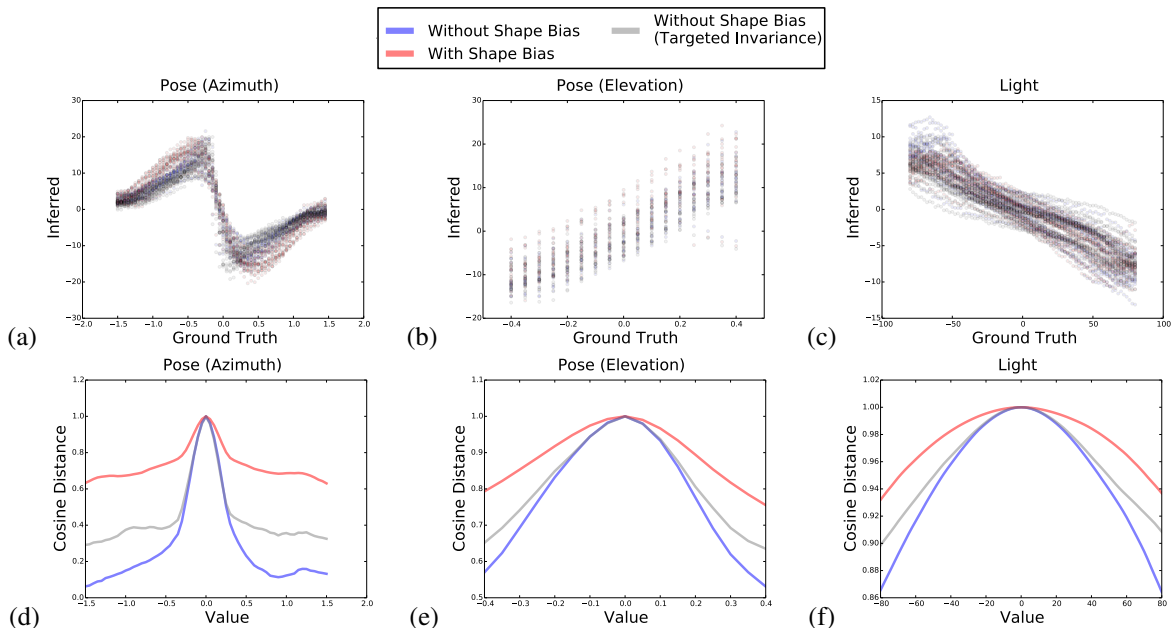


Figure 9: **Generalization of decoder to render images in novel viewpoints and lighting conditions:** We generated several datasets by varying light, azimuth and elevation, and tested the invariance properties of DC-IGN’s representation Z . We show quantitative performance on three network configurations as described in section 4.3. (a,b,c) All DC-IGN encoder networks reasonably predicts transformations from static test images. Interestingly, as seen in (a), the encoder network seems to have learnt a *switch* node to separately process azimuth on left and right profile side of the face. (d,e,f) We generated 100 faces and individually varied light, azimuth and elevation. Within each face set, we calculate the average cosine distance between the frontal face and every other transformed image. As demonstrated above, the network with strong shape bias has the strongest invariance power, which is intuitive as this network was trained using relatively higher facial variations. On the other hand, the *target invariance* training (without any shape bias) scheme gives stronger invariance in comparison to network trained without it.

4.3 Generalization of the rendering function

The decoder network learns an approximate rendering engine as shown in figure(8,10). Given a static test image, the encoder network produces the latents Z depicting scene variables such as light, pose, shape etc. Similar to an off-the-shelf rendering engine, we can selectively clamp z_i ’s and vary the rest. For example, as shown in figure 10, given the original test image, we can vary z_{light} by clamping all other nodes and conditionally generating the image through the decoder network. It is perhaps surprising that the learnt decoder network is able to approximately function like a 3D rendering engine. We performed similar analysis on other transformations as shown in figure 8.

We also quantitatively measured the decoder’s generalization capability to render across arbitrary viewpoints and lighting conditions. We generated 100 test batches from the 3DMM model where each batch contained a distinct face with varying pose (azimuth in range -1.5 to 1.5 with 0.05 step size). Within each batch, we compute the latent representation Z for every image and extracted the latents corresponding to face identity $z_{identity} \in z[4, n]$ as shown in figure 3. Within each batch, there is a face image with pose azimuth angle equal to zero (frontal image). For same face identity, we ideally expect $z_{identity}$ of all images within a batch to be equal. We calculated the co-

sine distance between the latent representation $z_{identity}$ of every image with the frontal image and averaged the score across all batches. As shown in figure 9(d), images close to the frontal face have almost identical latent representations but the similarity decays as azimuth goes away from zero. In other words, the invariance characteristics gradually degrades with viewpoint extrapolation. We perform similar analysis by generating separate datasets by varying elevation and lighting conditions.

We tested our model with three different DC-IGN network configurations – (1) DC-IGN with shape bias (see section 3.2), (2) DC-IGN without shape bias and (3) DC-IGN without shape bias but with targeted invariance (see section 3.2.1). All three networks do reasonably well in predicting azimuth, light and elevation (figure 9(a,b,c)). Interestingly, as shown in figure 9(a), the encoder network seems to have learnt a *switch* node to separately process left and right profile faces. However, as shown in figure 9(d,e,f), the network with high shape bias seems to have the strongest invariance properties. This intuitively makes sense as this network saw relatively larger variations in facial identities. It is also interesting to note (figure 9(a) and figure 8(b)) that in comparison to other transformations, generalization across the azimuth suffers most from radical extrapolation. This is likely because the lateral out-of-plane rotation transformation is probably one of the hardest trans-

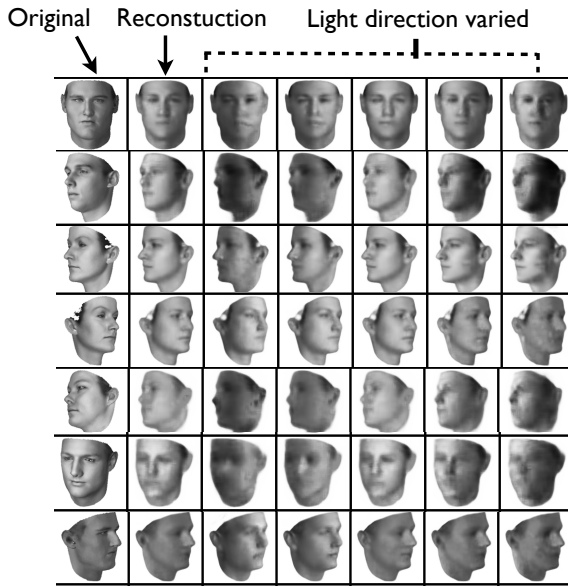


Figure 10: **Manipulating light variables:** Qualitative results showing the generalization capability of the learnt DC-IGN decoder to render original static image with different light directions. The latent neuron z_{light} is changed to random values but all other latents are clamped.

formations to learn for faces. However, this may improve by training the model with additional training data.

5 Discussion

We have shown that it is possible to train a deep convolutional inverse graphics network with interpretable graphics code layer representation just from raw images. By utilizing a deep convolution and de-convolution architecture within a variational autoencoder formulation, our model can be jointly trained using back-propagation using the stochastic variational objective function [12]. We proposed various training procedures to force the network to learn disentangled representations. Using 3D face analysis as a working example, we have demonstrated the invariant and equivariant characteristics of the learnt representation. Moreover, as highlighted in section 4.1, the DC-IGN deconvolutional network based decoder can be replaced by a domain-specific decoder for fine-grained model-based inference.

To scale our approach to handle more complex scenes, it will likely be important to experiment with deeper architectures in order to handle large number of object categories within a single network architecture. It is also very appealing to design a spatio-temporal based convolutional architecture to utilize motion in order to handle complicated object transformations. The current formulation of SGVB is restricted to continuous latent variables. However, real-world visual scenes contain unknown number of

objects that move in and out of frame. Therefore, it might be necessary to extend this formulation to handle discrete distributions. There has been recent work[15] on trying to approximate discrete distribution by using particle based variational approximations. An interesting future direction is to construct a mixed continuous-discrete variational approximation Q_{mixed} and to iteratively inter-leave optimization of the discrete parameters with SGVB.

We hope that our work motivates further research into automatically learning disentangled representations using variants of different encoder and decoder networks. The most general form of a decoder network can be thought of as a stochastic graphics program that conditions images given its latent *graphics code*. In the future, we aim to explore a hierarchy of coarse-to-fine encoder-decoder programs, where each encoder reasonably predicts a small set of latent variables and passes a noisy graphics code for the subsequent encoder-decoder program for refinement. This explicit hierarchy to sequentially handle different transformations may allow us to learn the network using relatively fewer training examples.

Acknowledgements

We thank Thomas Vetter for giving us access to the Basel face model. T. Kulkarni was graciously supported by the Leventhal Fellowship. This research was supported by ONR award N000141310333, ARO MURI W911NF-13-1-2012 and CBMM. We would like to thank Ilker Yildirim, Max Kleiman-Weiner, Karthik Rajagopal and Geoffrey Hinton for helpful feedback and discussions.

References

- [1] Y. Bengio. Learning deep architectures for ai. *Foundations and trends® in Machine Learning*, 2(1):1–127, 2009.
- [2] Y. Bengio, A. Courville, and P. Vincent. Representation learning: A review and new perspectives. *Pattern Analysis and Machine Intelligence, IEEE Transactions on*, 35(8):1798–1828, 2013.
- [3] Y. Bengio, E. Thibodeau-Laufer, G. Alain, and J. Yosinski. Deep generative stochastic networks trainable by backprop. *arXiv preprint arXiv:1306.1091*, 2013.
- [4] J. Bernardo, J. Berger, A. Dawid, A. Smith, et al. Regression and classification using gaussian process priors. In *Bayesian Statistics 6: Proceedings of the sixth Valencia international meeting*, volume 6, page 475, 1998.
- [5] V. Blanz and T. Vetter. A morphable model for the synthesis of 3d faces. In *Proceedings of the 26th annual conference on Computer graphics and interactive techniques*, pages 187–194. ACM Press/Addison-Wesley Publishing Co., 1999.
- [6] T. Cohen and M. Welling. Learning the irreducible representations of commutative lie groups. *arXiv preprint arXiv:1402.4437*, 2014.
- [7] A. Dosovitskiy, J. Springenberg, and T. Brox. Learning to generate chairs with convolutional neural networks. *arXiv:1411.5928*, 2015.

- [8] I. Goodfellow, H. Lee, Q. V. Le, A. Saxe, and A. Y. Ng. Measuring invariances in deep networks. In *Advances in neural information processing systems*, pages 646–654, 2009.
- [9] G. Hinton, S. Osindero, and Y.-W. Teh. A fast learning algorithm for deep belief nets. *Neural computation*, 18(7):1527–1554, 2006.
- [10] G. E. Hinton, A. Krizhevsky, and S. D. Wang. Transforming auto-encoders. In *Artificial Neural Networks and Machine Learning–ICANN 2011*, pages 44–51. Springer, 2011.
- [11] V. Jampani, S. Nowozin, M. Loper, and P. V. Gehler. The informed sampler: A discriminative approach to bayesian inference in generative computer vision models. *arXiv preprint arXiv:1402.0859*, 2014.
- [12] D. P. Kingma and M. Welling. Auto-encoding variational bayes. *arXiv preprint arXiv:1312.6114*, 2013.
- [13] A. Krizhevsky, I. Sutskever, and G. E. Hinton. Imagenet classification with deep convolutional neural networks. In *NIPS*, pages 1106–1114, 2012.
- [14] T. D. Kulkarni, V. K. Mansinghka, P. Kohli, and J. B. Tenenbaum. Inverse graphics with probabilistic cad models. *arXiv preprint arXiv:1407.1339*, 2014.
- [15] T. D. Kulkarni, A. Saeedi, and S. Gershman. Variational particle approximations. *arXiv preprint arXiv:1402.5715*, 2014.
- [16] Y. LeCun and Y. Bengio. Convolutional networks for images, speech, and time series. *The handbook of brain theory and neural networks*, 3361, 1995.
- [17] H. Lee, R. Grosse, R. Ranganath, and A. Y. Ng. Convolutional deep belief networks for scalable unsupervised learning of hierarchical representations. In *Proceedings of the 26th Annual International Conference on Machine Learning*, pages 609–616. ACM, 2009.
- [18] M. M. Loper and M. J. Black. Opendr: An approximate differentiable renderer. In *Computer Vision–ECCV 2014*, pages 154–169. Springer, 2014.
- [19] V. Mansinghka, T. D. Kulkarni, Y. N. Perov, and J. Tenenbaum. Approximate bayesian image interpretation using generative probabilistic graphics programs. In *Advances in Neural Information Processing Systems*, pages 1520–1528, 2013.
- [20] J. Masci, U. Meier, D. Cireşan, and J. Schmidhuber. Stacked convolutional auto-encoders for hierarchical feature extraction. In *Artificial Neural Networks and Machine Learning–ICANN 2011*, pages 52–59. Springer, 2011.
- [21] I. Murray, R. P. Adams, and D. J. MacKay. Elliptical slice sampling. *arXiv preprint arXiv:1001.0175*, 2009.
- [22] V. Nair, J. Susskind, and G. E. Hinton. Analysis-by-synthesis by learning to invert generative black boxes. In *Artificial Neural Networks–ICANN 2008*, pages 971–981. Springer, 2008.
- [23] P. Paysan, R. Knothe, B. Amberg, S. Romdhani, and T. Vetter. A 3d face model for pose and illumination invariant face recognition. *Proceedings of the 6th IEEE International Conference on Advanced Video and Signal based Surveillance (AVSS) for Security, Safety and Monitoring in Smart Environments*, 2009.
- [24] R. Salakhutdinov and G. E. Hinton. Deep boltzmann machines. In *International Conference on Artificial Intelligence and Statistics*, pages 448–455, 2009.
- [25] Y. Tang, R. Salakhutdinov, and G. Hinton. Deep lambertian networks. *arXiv preprint arXiv:1206.6445*, 2012.
- [26] T. Tieleman. *Optimizing Neural Networks that Generate Images*. PhD thesis, University of Toronto, 2014.
- [27] A. Vedaldi and K. Lenc. Matconvnet – convolutional neural networks for matlab. *CoRR*, abs/1412.4564, 2014.
- [28] P. Vincent, H. Larochelle, I. Lajoie, Y. Bengio, and P.-A. Manzagol. Stacked denoising autoencoders: Learning useful representations in a deep network with a local denoising criterion. *The Journal of Machine Learning Research*, 11:3371–3408, 2010.
- [29] R. D. Wilkinson. Approximate bayesian computation (abc) gives exact results under the assumption of model error. *Statistical applications in genetics and molecular biology*, 12(2):129–141, 2013.
- [30] I. Yildirim, T. Kulkarni, W. Freiwald, and J. Tenenbaum. Explaining monkey face patch system as deep inverse graphics. In *Computational and Systems Neuroscience*, 2015.
- [31] M. D. Zeiler, D. Krishnan, G. W. Taylor, and R. Fergus. Deconvolutional networks. In *Computer Vision and Pattern Recognition (CVPR), 2010 IEEE Conference on*, pages 2528–2535. IEEE, 2010.